NUMERICAL ANALYSIS OF THE EUTECTIC MELTING AND RELOCATION OF THE B_4C CONTROL ROD MATERIALS BY THE MPFI-MPS METHOD

Shota Ueda*, Masahiro Kondo† and Koji Okamoto‡

* Nuclear Technology Research Laboratory
Central Research Institute of Electric Power Industry (CRIEPI)
2-6-1 Nagasaka, Yokosuka-shi, Kanagawa 240-0196, Japan
e-mail: ueda3745@criepi.denken.or.jp - Web page: https://criepi.denken.or.jp/en/index.html
(Formerly, the University of Tokyo)

† National Institute of Advanced Industrial Science and Technology (AIST)
1-1-1 Umezono, Tsukuba, Ibaraki 305-8568, Japan
e-mail: kondo.masahiro@aist.go.jp - Web page:
https://unit.aist.go.jp/cd-fmat/ja/teams/igms.html

‡ Nuclear Professional School
The University of Tokyo
2-22 Shirakata, Tokai-mura, Ibaraki 319-1188, Japan
e-mail: okamoto@n.t.u-tokyo.ac.jp - Web page: http://www.utvis.com

Key words: Eutectic melting, MPS, MPFI, Boron-carbide control rod, Severe accident

Abstract. Eutectic melting and subsequent relocation of the boron-carbide (B_4C) control rod materials were simulated by a particle method. In the past, it was difficult to simulate the eutectic melting by a particle method because the melting starts at the interface between two different materials, which leads to the instability of the particle motion due to the small amount of fluid particles and lack of the thermodynamic consistency of the particle system. Thus, the Moving Particle Full Implicit (MPFI)-Moving Particle Semi-implicit (MPS) method was developed and introduced in the current study. Specifically, the MPFI method was introduced for the momentum transfer calculation, and the MPS method was introduced for the heat and mass transfer calculation. The MPFI-MPS method realized the simulation of the eutectic melting and subsequent relocation behaviour.

1 INTRODUCTION

In Fukushima decommissioning, investigation of the boron distribution in the fuel debris is of great significance because it affects the risk of re-criticality[1]. The major source

for the boron species is the boron-carbide B_4C control rod. Thus, the eutectic melting and relocation behavior of B_4C control rod materials receive remarkable attention.

Eutectic melting can occur at the contact interface of several chemical components at lower temperature than melting points of each pure material. B_4C and stainless steel (SS) can have eutectic melting[2] in the B_4C control rod. Liquid phase suddenly appears at the solid interface in eutectic melting, and the complicated multi-component interactions and surface deformation occur. which are challenging for Eulerian direct numerical simulation methods. A particle method, which is one of the Lagrangian methods, is suitable for simulating such complicated flows because it can easily track the motion of thermo-physical properties of eutectic melting, inclusive of solid/liquid phase changes. The Moving Particle Semi-implicit method developed by Koshizuka and Oka[3, 4] is one of such particle methods for the incompressible free surface fluid flow. Eutectic melting model was also developed in MPS framework[5]. However, it was difficult to calculate the initial formation of the liquid phase between the solid phases due to eutectic melting. It is often because the instability of pressure calculation is caused by the too small number of liquid particles between solid phases just after eutectic melting started. Suppressing the numerical oscillations in pressure calculation solves this issue in some cases[6]. Meanwhile, it was reported that modeling a solid phase as very high-viscous fluid can solve the issue because it virtually increases the number of fluid particles used for the pressure calculation[7]. The Moving Particle Full Implicit method[8] is one of the promising method for this kind of issues related with the instability. The MPFI method inherently suppresses the instability of the particle motion because it assures thermodynamic consistency of the particle system after discretization. Thus, it may be expected that adopting the MPFI method [8] for the momentum transfer calculation, and the MPS method [3, 4] for the heat and mass transfer calculation can enjoy the benefits from both the methods to simulate eutectic melting and subsequent relocation; stable calculation and smooth distribution of physical values.

In this study, eutectic melting and subsequent relocation of the B_4C control rod materials were simulated by a particle method. The MPFI-MPS method was developed and introduced in the current simulation. The eutectic melting and relocation processes of the control rod materials were discussed.

2 NUMERICAL METHOD

In this study, we adopted the MPFI method [8] for the momentum transfer calculation, and the MPS method [3, 4] for the heat and mass transfer calculation. The MPFI method suppresses the instability of the particle motion because it assures thermodynamic consistency of the particle system after discretization. Moreover, it conserves angular momentum and makes it possible to simulation rotational motion of fluid. Meanwhile, the heat and mass transfer calculation by the MPS method offers smooth distribution of physical values. We call this method the MPFI-MPS method. In the MPFI method, the particle

interaction models for gradient, divergence and Laplacian operators are formulated as:

$$\nabla\phi = \sum_j (\phi^j + \phi^i)\boldsymbol{r}^{ij}\frac{w'^{ij}}{d^{ij}}, \tag{1}$$

$$\nabla \bullet \boldsymbol{A} = \sum_j (\boldsymbol{A}^j - \boldsymbol{A}^i)\boldsymbol{r}^{ij}\frac{w'^{ij}}{d^{ij}} \tag{2}$$

and

$$\nabla^2\phi = \sum_j (\phi^j - \phi^i)\frac{w'^{ij}}{d^{ij}}. \tag{3}$$

where w'^{ij} is the differential of the weight function shown in Eq. 4:

$$w(d) = \begin{cases} \frac{(r_e - d^{ij})^2}{n_0} & (0 \le r \le r_e) \\ 0 & (r_e \le r) \end{cases} \tag{4}$$

where r_e is an effective radius and d^{ij} is a particle distance. n_0 is a constant to standardize the weight function. The weight function of Eq. 4 is used in the MPFI method. The differential of this weight function is non-zero at $d^{ij} = 0$ so as to keep the particle arrangement uniform.

The following governing equation was adopted:

$$\rho\frac{du_i}{dt} = \frac{\partial}{\partial x_j}\mu\dot{\varepsilon_{ij}} + \frac{\partial}{\partial x_i}(\lambda\dot{\varepsilon_{kk}} + \kappa\varepsilon_{kk}) + \rho g_i. \tag{5}$$

Since this equation becomes the well-known form of incompressible NS equation when we set the parameters λ and κ large enough, it can be used instead of the incompressible NS equation. The first term on the right-hand side is the viscosity term and the second term is equivalent to the pressure term in the general NS equation. Here, the pressure is expressed as:

$$P = -(\lambda\dot{\varepsilon_{kk}} + \kappa\varepsilon_{kk}). \tag{6}$$

The details of the MPFI method are described in the literature [8].

In the MPFI method, the particle interaction models for gradient, divergence and Laplacian operators are formulated as:

$$\nabla\phi_i = \frac{d}{n^0}\sum_{j\neq i}\frac{(\phi_j - \phi_i)(\boldsymbol{r}_j - \boldsymbol{r}_i)}{|\boldsymbol{r}_j - \boldsymbol{r}_i|^2}w(|\boldsymbol{r}_j - \boldsymbol{r}_i|) \tag{7}$$

$$\nabla \cdot \boldsymbol{\phi}_i = \frac{d}{n^0}\sum_{j\neq i}\frac{(\boldsymbol{\phi}_j - \boldsymbol{\phi}_i)\cdot(\boldsymbol{r}_j - \boldsymbol{r}_i)}{|\boldsymbol{r}_j - \boldsymbol{r}_i|^2}w(|\boldsymbol{r}_j - \boldsymbol{r}_i|) \tag{8}$$

$$\nabla^2\phi_i = \frac{2d}{\lambda n^0}\sum_{j\neq i}[(\phi_j - \phi_i)(w(|\boldsymbol{r}_j - \boldsymbol{r}_i|)] \tag{9}$$

$$\lambda = \frac{\sum_{j\neq i}|\boldsymbol{r}_j - \boldsymbol{r}_i|^2 w(|\boldsymbol{r}_j - \boldsymbol{r}_i|)}{\sum_{j\neq i} w(\boldsymbol{r}_j - \boldsymbol{r}_i)} \tag{10}$$

where, d, n^0 and w denote spatial dimensions and a particle number density. λ is a coefficient to make the statistic increase of deviation consistent to an analytical solution. w denotes the weight function defined as:

$$w(r) = \begin{cases} \frac{r_e}{r} - 1 & (0 \leq r \leq r_e) \\ 0 & (r_e \leq r) \end{cases} \tag{11}$$

where, r denotes a particle distance.
In this study, melting and solidification behavior is expressed with the viscosity change. The solid SS and solid B_4C were modeled as a very high-viscous fluid.

The temperature field is calculated with the heat transfer equation:

$$\frac{Dh}{Dt} = k\nabla^2 T + Q \tag{12}$$

Here, h denotes enthalpy, T denotes temperature, k denotes thermal conductivity and Q denotes heat source. To estimate the temperature from enthalpy, linear relationship between them was assumed in this study. The latent heat was considered with temperature recovery method [9]. Eutectic melting model in the literatures[5, 6] was adopted in the current study. It is mainly composed of two procedures; solving diffusion equation with respect to B_4C and determining the phase of a particle based on Fe–B binary phase diagram. The phase diagram decides whether a particle is solid or liquid by referring to its temperature and mass fraction of B_4C to SS. We assumed that no volumetric change occurs due to the phase change.

3 CALCULATIONS

The eutectic melting of the control-rod materials was simulated in a three-dimensional way to understand their relocation behavior. Figure 1 shows the calculation geometry and initial condition used in the simulation. Two calculation bodies were set in the calculation region. The rod-shaped body at the center (Specimen region) represents the simulated control rod with the physical properties of the control-rod materials. The plates at the sides of the specimen region represent tungsten heaters (W heaters). Thermal radiation was calculated by the S2S thermal radiation model in the simulation. Solid SS and solid B_4C were modeled as a very high-viscous fluid. The bottom half of the specimen was treated with the wall particles. The temperature of heaters was set at 2473 K in this case. The emissivity of the materials was set at 0.23.

Table 1 shows the physical properties used in this study. Here, T denotes the temperature of a particle. The thermal conductivity of B_4C powder bed at the filling rate of 76% was used.

Figure 2 is a representation of solid/liquid particles with respect to viscosity at 60–77 s in a front view. Figure 3 is a front sectional view of Figure 2. The melting at the B_4C-SS interface was successfully calculated. The eutectic melting started from the interface. It was kept inside the specimen until it melted through the SS cladding. After that, it flew down along the SS surface. It was observed that the outer surface of the SS cladding was molten after the contact of the spreading melt (see Figure 3). Some of the eutectic melt solidified because its shape changed while flowing down and heat release to the environment overwhelmed the heat absorption there. Figure 4 and Figure 5 show temperature distribution at 0–68 s and 68–77 s in a front view. The temperature on a upper part of the rod increased by the thermal radiation from the tungsten heaters while that on its bottom part decreased due to the heat release to the environment by thermal radiation. The temperature distribution has approached almost equilibrium before the eutectic melting started. Figure 6 and Figure 7 show B_4C distribution at 0–68 s and 68–77 s in a front view. The B_4C was transferred into the pure SS cladding. In this simulation, temperature distribution reached the steady state firstly, and afterward the rod started to melt when the Fe-B composition in a part of the rod reached the enough value to form a liquid phase in the Fe-B binary phase diagram. The viscosity of the melted part decreased, while that of the solid part remained at the initial high viscosity (Figure 2). The results imply that the eutectic melting from the outer surface of the SS cladding governs the melting speed of the control rod after the eutectic melt penetrates the SS cladding and flow out.

Table 1: Calculation conditions for simulation

Initial particle distance	5.0×10^{-4} m
Density of SS [10]	7.90×10^3 kg/m^3
Density of B_4C[10]	$2.52 \times 10^3/1.33$ kg/m^3
Specific heat capacity of SS[10]	$326.0 - 0.242T + 3.71T^{0.719}$ J/kg/K
Specific heat capacity of B_4C[10]	$563.0 + T(1.54 - 2.94 \times 10^{-4} \times T)$ J/kg/K
Thermal conductivity of SS[10]	$7.58 + 0.0189T$ W/m/K
Thermal conductivity of B_4C[10]	$4.60 + 0.00205T + 26.5\exp(-\frac{T}{448.0})$ W/m/K
Latent heat of fusion	1929 mJ/mm^3
Inter-diffusion coefficient	$2.00 \times 10^{-07}\exp(-\frac{21000\times4.184}{8.3\times T})$ m^2/s
Kinematic viscosity of eutectic melt	1.0 mPa·s
Gravity	9.81 m/s^2

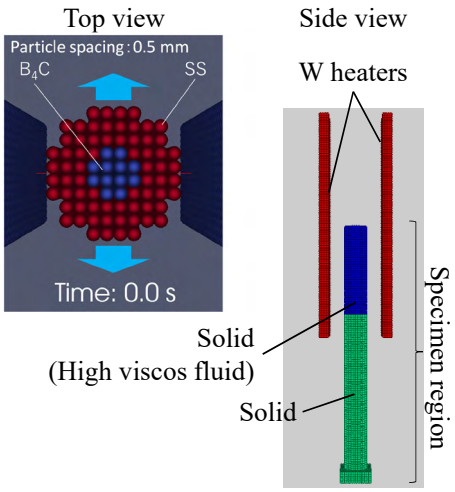

Figure 1: Calculation geometry and conditions in three-dimensional simulation.

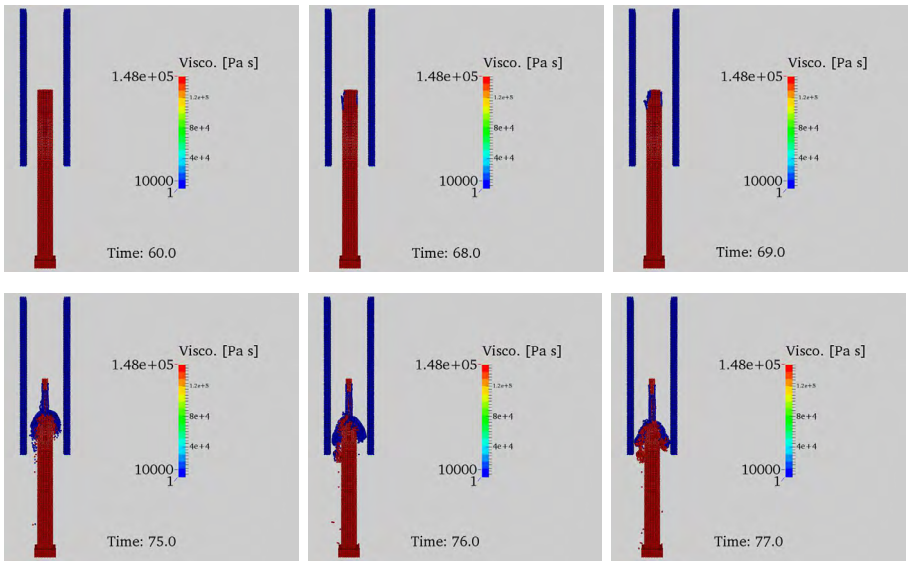

Figure 2: Representation of solid/liquid particles with respect to viscosity at 60–77 s (front view).

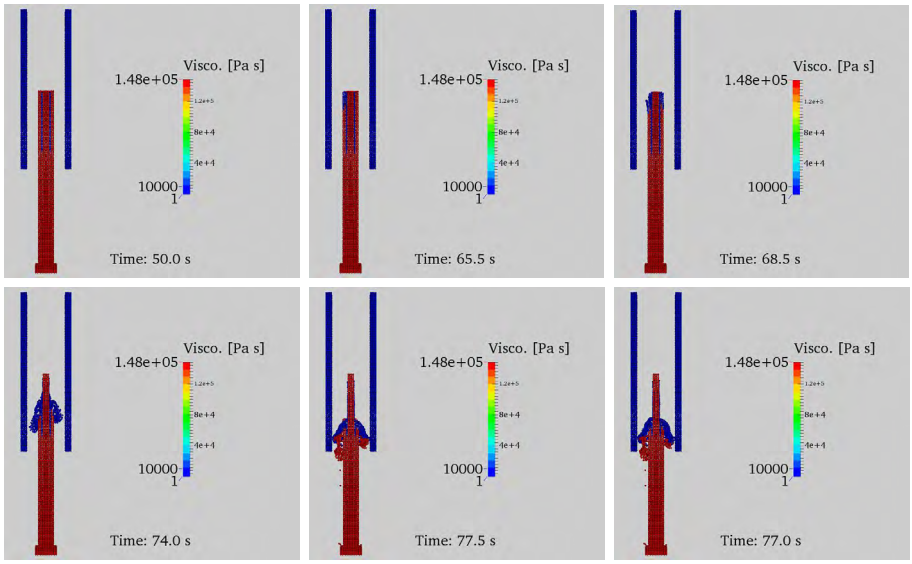

Figure 3: Representation of solid/liquid particles with respect to viscosity at 50–77 s (front sectional view).

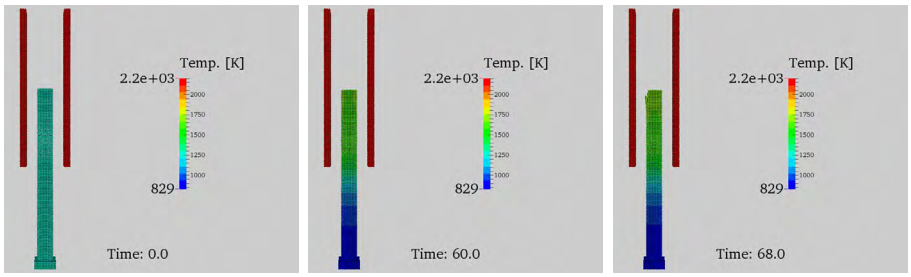

Figure 4: Temperature distribution at 0–68 s (front view).

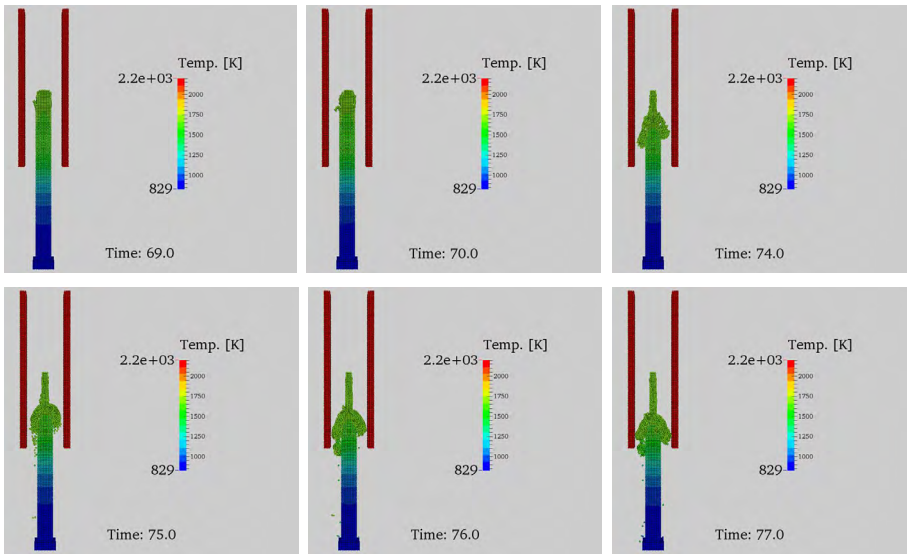

Figure 5: Temperature distribution at 68–77 s (front view).

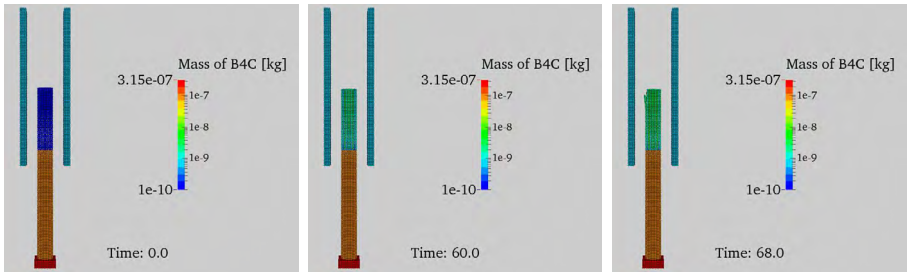

Figure 6: B_4C distribution with respect to mass [kg] at 0–68 s (front view).

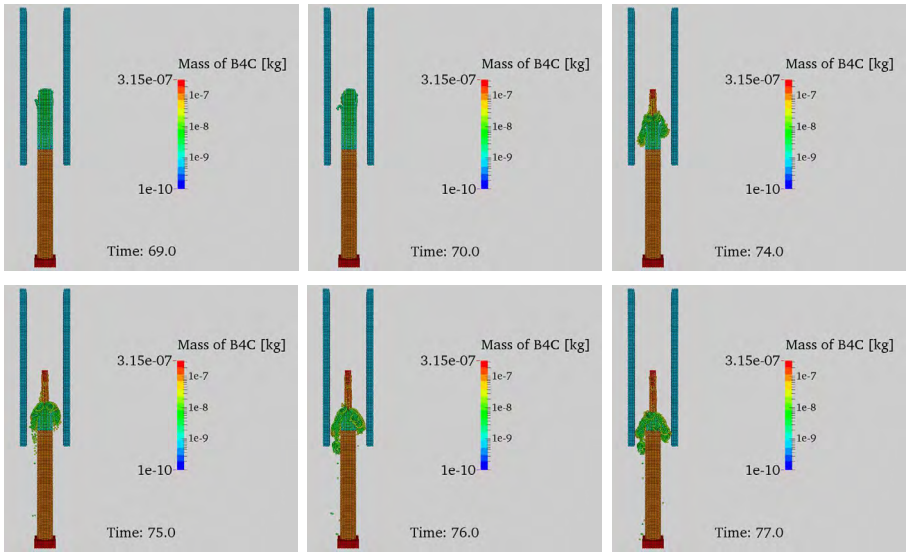

Figure 7: B_4C distribution with respect to mass [kg] at 69–77 s (front view).

4 CONCLUSIONS

Eutectic melting and subsequent relocation of the B_4C control rod materials were simulated by a particle method. The MPFI-MPS method was developed and introduced in the current simulation. The numerical analysis of the specimen which simulates the partial length of the B_4C control rod suggested that dominant eutectic-melting interfaces changes before and after the eutectic melting reaches the specimen surface.

ACKNOWLEDGMENTS

Funding: This study was partially supported by JSPS KAKENHI Grant Number 17J07634 and "High-accuracy computations of the core structure relocation during severe accidents" project funded by the Initiatives for Atomic Energy Basic and Generic Strategic Research Program of the Ministry of Education, Culture, Sports, Science and Technology of Japan.

REFERENCES

[1] Kasada, R., HA, Y., Higuchi, T. and Sakamoto, K., 2016. Chemical State Mapping of Degradated B4C Control Rod Investigationwith Soft-X-ray Emission Spectrometer in Electron Probe Micro-analysis, *Scientific Reports*, **6**, Article number: 25700.

[2] Gauntt, R., Gasser, R. and Ott, L. J. The DF-4 fuel damage experiment in ACRR with a BWR control blade and channel box. Washington, DC: Division of Systems Research, Office of Nuclear Regulatory Research, U.S. Nuclear Regulatory Commission; 1989, SAND86-1443, NUREG/CR-4671.

[3] Koshizuka, S., Oka, Y. 1996. Moving particle semi-implicit method for fragmentation of incompressible fluid. *Nuclear Science and Engineering*, **123**(3) 421-434.

[4] Koshizuka, S., Shibata, K., Kondo, M. and Matsunaga, T. 2018. Moving Particle Semi-implicit Method: A Meshfree Particle Method for Fluid Dynamics. London: Academic Press.

[5] Mustari, A.P.A., Oka, Y., 2014. Molten uranium eutectic interaction on iron-alloy by MPS method. *Nucl. Eng. Des.* **278**, 387394. doi:10.1016/j.nucengdes.2014.07.028.

[6] Ueda, S., Madokoro, H., Kondo, M. and Okamoto, K., 2018. Numerical Analysis on Eutectic Melting of Boron Carbide Control Rod Materials with a Particle Method. *Transactions of JSCES*, Paper No. 20182002 [In Japanese].

[7] Nagatake, T., Yoshida, H., Takase, K., and Kurata, M., 2015. Development of popcorn code for simulating melting behavior of fuel element; fundamental validation and simulation for melting behavior of simulated fuel rod. Proc. of 23rd Int. Conf. on Nuclear Engineering, Chiba, Japan, May, pp. 1–6.

[8] Kondo, M., Ueda, S. and Okamoto, K., 2017. Melting Simulation Using a Particle Method with Angular Momentum Conservation. 2017 25th International Conference on Nuclear Engineering, July 2–6, Shanghai, China.

[9] Ohnaka, I. 1985. Introduction to Computational Heat Transfer and Solidification Analysis–Application to Casting Process. Tokyo: Maruzen co. [in Japanese]

[10] Siefken, L.J., Coryell, E.W., Harvego, E.A., Honorst, J.K., Matpro -A Library of Materials Properties for Light-Water-Reactor Accident Analysis, Washington, DC: Division of Systems Research, Office of Nuclear Regulatory Research, U.S. Nuclear Regulatory Commission; 2001, NUREG/CR-6150.